



Isolation of interfacially active molecules from Brazilian oils and characterization by high resolution analytical techniques

Wanderson Romão^{1,2} · Eliane V. Barros^{1,2} · Natã C. L. Madeira¹ · Luiz S. Chinelatto Jr.³ · Marcia C. K. de Oliveira³ · Valdemar Lacerda Jr.¹

Received: 10 October 2022 / Revised: 7 April 2023 / Accepted: 13 April 2023 / Published online: 15 May 2023
© The Author(s) under exclusive licence to Associação Brasileira de Engenharia Química 2023

Abstract

Some petroleum molecules with interfacial activity play a fundamental role in stabilizing water-in-crude oil (W/O) emulsions, leading to significant flow assurance challenges during oil production and thus are the focus of this study. Using the wet silica method, three crude oils from Brazilian fields were fractionated into two fractions: one containing the interfacially active molecules (IM) and the other containing the non-interfacially active molecules (the so-called clean up (CU) fraction), which are adsorbed onto silica in this method. Nuclear Magnetic Resonance (NMR) essays of the oils provided the molecular parameters, such as average linear chain length, bridgehead carbons and aromatic hydrogens. The characterization of IMs, CUs and their parent oils by high resolution and precision mass spectrometry (FT-ICR MS) showed the influence of total acid number (TAN) in the percentage of O₂[H] class found, but no clear differences were found between the chemical composition of the IMs isolated. The IMs were rich in O₃S[H] class, presumably of natural origin. The characterization results and the dynamic surface tension measurements can help in the development of chemical products with high performance in the treatment of W/O emulsions.

Keywords Water-in-crude oil emulsions · Interfacially active molecules · ESI(±)FT-ICR MS · NMR

Introduction

During crude oil production, a considerable amount of water is inevitably produced, leading to the formation of water-in-crude oil (W/O) emulsions and, in some cases, severe production losses. The presence of water in crude oil will also reduce the quality of the crude oil itself, increase the operating costs due to the need to separate emulsions, lead to corrosion problems, and also can cause contamination

of catalysts used in the refining process (Wong et al. 2015). Indeed, variations in production parameters such as temperature, pressure, pH and water cut affect the partitioning of surfactant molecules present in the W/O system, such as naphthenic acids in produced water (Bertheussen et al. 2018). The results of different studies suggest that constituents of crude oil, such as resins, naphthenic acids, and asphaltenes, are the main components of crude oil responsible for the formation of robust interfacial films that stabilize W/O emulsions (Czarnecki et al. 2012; Spiecker et al. 2003; Mahavadi et al. 2022; Facanali et al. 2021; Tchoukov et al. 2014; Ese and Kilpatrick 2004; Li et al. 2023). The stability of an emulsion mainly depends on the interaction between dissolved or colloidal particles in both phases, from surfactants, fine solids, polymers and electrolytes. Emulsions are stable due to the existence of small drops of the dispersed phase and the presence of an interfacial film that surrounds the drops (Ese and Kilpatrick 2004). Furthermore, there is clear evidence of a multi-factor synergistic emulsification stabilization mechanism (Li et al. 2022). Despite this multi-factor stabilization mechanism, from a thermodynamic point of view, emulsions are unstable systems, since there

This is an invited, extended version of the manuscript presented in the 1st Flow Assurance, Technology Congress and published in the FATC22 Anais.

✉ Luiz S. Chinelatto Jr.
lsilvino@petrobras.com.br

¹ Chemistry Department, Federal University of Espírito Santo, Vitória, ES, Brazil

² Federal Institute of Education, Science and Technology of Espírito Santo, Vitória, ES, Brazil

³ Research, Development and Innovation Center, PETROBRAS, Rio de Janeiro, RJ, Brazil

is a natural tendency for a liquid–liquid system to separate and reduce its interfacial energy. Effective ways to treat W/O emulsions demand a deep knowledge of the chemical structure of molecules responsible for stabilizing them. Understanding the properties of oil–water interfacial films as well as the molecules involved in emulsion stabilization provides fundamental insights into the design and synthesis of specialty chemical emulsifiers and demulsifiers, even for unconventional oil reserves (about 70% of total world oil) such as heavy oil, oil/tar sands and shale oil (He et al. 2015).

On the other hand, the low content (1%wt) of interfacially active molecules in the W/O emulsions interface (IM) makes it difficult to elucidate the chemical composition from its varied, complex matrix (Lalli et al. 2017). Thus, the characterization of those species includes the application of preliminary methods for IM isolation.

Over the years, many methods have been used for the isolation of fractions containing petroleum components with interfacial affinity, including centrifugation at different rotation speeds, times and temperatures, and with different extraction techniques, such as the heavy water method, the Wu method (which also involves a centrifuge step (Wu 2003)) and sequential redissolution of asphaltenes dispersed in polytetrafluoroethylene granules (Schabron et al. 2010). All these methods have in common the fact that they are laborious, difficult, or impractical for the generation of sufficient quantities of IM (tens of milligrams) that are also free from petroleum compounds without interfacial activity. In some cases, the loss of volatiles during IM isolation is an additional problem, making it difficult or impossible to use the method on medium and light density oils.

Jarvis et al. (2015), proposed an IM separation method called the wet silica method, considered by the authors as fast, easy to implement, efficient and applicable to light, medium and heavy oils, in addition to being scalable. The authors added IM that had been isolated by the wet silica method to a model system; such addition effectively resulted in the formation of a stable emulsion for the model system, validating the method. Lalli et al. (2017) added a standard mixture of alkylbenzenesulfonates (surfactants) to the oil, reaffirming the efficiency of the wet silica method (the IM obtained by the wet silica method was rich in such surfactants). Due to these characteristics, the wet silica method was chosen in the present work, notably because of its potential to generate quantities of IM greater than 10 mg and free from significant amounts of contaminants. Similarly, Silva et al. (2020) applied the wet silica technique for IM extraction from crude oil samples of Brazilian fields. The authors observed a significant reduction in the interfacial tension values of the IM fraction in relation to its original oil, in a brine/organic solution model system. The characterization of the IM by Fourier transform infrared spectroscopy (FTIR) and proton nuclear magnetic resonance

(^1H NMR) revealed the polar and aromatic character of the IM fractions, adsorbed onto the hydrophilic surface of the silica particles, and the predominance of hydrocarbons in the fraction containing the non-adsorbed molecules. The Fourier transform ion cyclotron resonance mass spectrometry (FT-ICR-MS) data showed that most of the acid classes in the IM were dependent on the corresponding oil sample and were independent of the solvent system.

Due to the complexity and variety of different crude oils, much research is still necessary to identify the chemical structure of the IM to allow structure–property correlation and advances in the optimization of the petroleum production process. In this study, the wet silica method introduced by Jarvis et al. (2015) was applied to the isolation of IM from two medium oils (Oil 1 and Oil 2) and one heavy crude oil (Oil 3) from Brazilian fields to understand their role in crude oil emulsion stability.

Materials and methods

Materials

Crude oil samples were supplied by PETROBRAS. Reagent grade toluene, methanol, n-heptane, formic acid and ammonium hydroxide were purchased from Vetec Química Fina Ltd., Rio de Janeiro, Brazil. Chromium-(III) acetylacetonate (~98%), arginine (≥ 98), carbon disulfide (≥ 99.9), and C_2Cl_4 ($\geq 99\%$); were obtained from Sigma-Aldrich-Merck. Chloroform-D (D, 99.8%) was obtained from Cambridge Isotope Laboratories. NaCl and CaCl_2 were obtained from Sigma Aldrich, San Luis, USA. All chemicals were used without further purification.

Methods

Crude oil assay

The separation of the saturate, aromatic, resin and asphaltene fractions (SARA analysis) was carried out using a modified version of the thin layer chromatography–flame ionization detection (TLC–FID) method. In this procedure, asphaltenes were separated and quantified by the ASTM D6560-17 method. Another portion of the same petroleum sample was separated by microdistillation into $< 260\text{ }^\circ\text{C}$ and $> 260\text{ }^\circ\text{C}$ fractions. Supercritical fluid chromatography using carbon disulfide separated the $< 260\text{ }^\circ\text{C}$ fraction into saturates (S1) and aromatics (A1). In parallel, the $> 260\text{ }^\circ\text{C}$ fraction was fractionated by TLC–FID into the heavier saturates (S2), aromatics (A2), and the polar compounds (P). S1 + S2 corresponded to the saturates, A1 + A2 to the aromatics, and the polar compounds minus the asphaltenes corresponded to the resins. API gravity and density, total acid number

(TAN) value and water content were determined according to the methods ISO 12185–96, ASTM D664-18 and ASTM D4377-20, respectively.

Dynamic surface tension

NaCl and CaCl₂ were used to prepare four saline solutions with different concentrations and pHs as follows: Brine 1) 2 g L⁻¹ of CaCl₂ and 50 g L⁻¹ of NaCl, pH 6; Brine 2) 2 g L⁻¹ of CaCl₂ and 50 g L⁻¹ of NaCl, pH 8; Brine 3) 5 g L⁻¹ of CaCl₂ and 110 g L⁻¹ of NaCl, pH 6; Brine 4) 5 g L⁻¹ of CaCl₂ and 110 g L⁻¹ of NaCl, pH 8. Deionized water was obtained through a Thermo Scientific Nano Pure™ purification system with a resistivity of 18.2 MΩ cm⁻¹ at 25 °C. The pH of the solutions was adjusted with 0.1 M NaOH solution. The brines were prepared to study both the effect of salinity and the effect of pH at the water–oil interface. All measurements were performed at a fixed temperature of 23 ± 0.1 °C. The salt content and pH of the brines are shown in Table 1.

The dynamic interfacial tension of water in crude oil was measured using the pendant drop technique (Berry et al. 2015) on a tensiometer (Attension Theta, BiolinScientific, see Fig. 1a) to elucidate the adsorption kinetics of

active interfacial materials at the water/oil interface. A 22 gauge hook needle was connected to a 200 μL Hamilton syringe and filled with a 10 g L⁻¹ oil/toluene solution. The syringe was then fixed above a cubic, quartz cuvette filled with deionized water and different brines (Fig. 1b). A drop of oil with an approximate volume of 18 μL was generated through the needle, which was immersed in the aqueous phase while the drop remained attached to the needle. The interfacial tension (IFT) recording was calculated according to the Young–Laplace equation, and videos were recorded using the equipment software. Laplace's Eq. (1) relates the change in surface pressure separating two distinct liquids to molecular bonding forces. In its most general form, it can be expressed as:

$$\Delta p = \gamma(1/R_1 + 1/R_2) \quad (1)$$

where Δp is the change in pressure between the surfaces, γ is surface tension and R is the two-perpendicular radius of curvature. Therefore, the smaller the drop radius, the greater the pressure difference of its surface. The Young–Laplace equation also reveals that liquids with concave surfaces (i.e., a negative radius of curvature) have lower pressures compared to flat surfaces (an infinite radius of curvature), and that both these types of surfaces have lower pressures than convex surfaces (with a positive radius of curvature).

Table 1 Saline solution compositions

Brine	*pH	Cations		Anion
		Na ⁺ (g L ⁻¹)	Ca ²⁺ (g L ⁻¹)	Cl ⁻ (g L ⁻¹)
1	6	50	2	54
2	8	50	2	54
3	6	110	5	120
4	8	110	5	120

*pH was adjusted with 0.1 M NaOH solution

Nuclear magnetic resonance (NMR)

Solution-state ¹³C NMR spectra were recorded at 9.40 T on an Agilent 400 NMR spectrometer, operating at 100.44 MHz, using a 10 mm probe. Samples were dissolved at 20 wt % in 0.05 M chromium (III) acetylacetonate (as the relaxation agent) in chloroform-D (CDCl₃). The following experimental conditions were used: 25.0 kHz spectral width, 10.2 μs (90°)

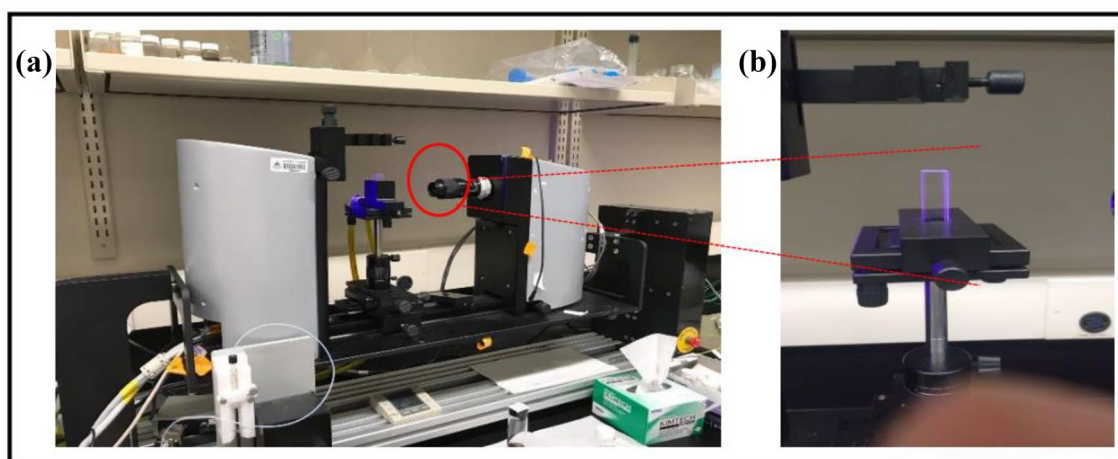


Fig. 1 a Tensiometer and b quartz cuvette

rf pulses, 1.3 s acquisition time and 7 s pulse delay. 5000 scans were accumulated. The nuclear Overhauser enhancement was suppressed by operating the spectrometer in the “inverse-gated” mode where the broad-band proton decoupling was turned on only during acquisition periods. Solution state ^1H NMR spectra were recorded at 11.75 T on a Bruker Avance III 500 spectrometer, operating at 500.18 MHz, using a 5 mm probe. Samples were dissolved at 5 wt % in $\text{CDCl}_3:\text{C}_2\text{Cl}_4$ (1:1 v/v). The following experimental conditions were used: 10.0 kHz spectral width, 3.3 μs (30°) rf pulses, 2.3 s acquisition time, 1 s pulse delay, and 128 scans were accumulated. All experiments (^1H and ^{13}C) were performed at 32°C .

Electrospray ionization FT-ICR mass spectrometry (ESI(\pm) FT-ICR MS)

The samples of crude oil and the fractions were analyzed by mass spectrometry using a 9.4 T Q-FT-ICR MS hybrid device (Solarix, Bruker Daltonics, Bremen, Germany) equipped with a commercially available ESI source (Bruker Daltonics). The dynamic operating range for ion acquisition in the ICR cell was configured to m/z 200–1500. All samples (oils, CUs and IMs) were diluted to approximately 1.5 mg/mL in a 1:1 (v/v) toluene/methanol solution containing 0.1% (v/v) formic acid or ammonium hydroxide for analysis in ESI(+) and ESI(–) modes, respectively. Each solution was injected by direct infusion at a flow of 5 $\mu\text{L}/\text{min}$. Each spectrum was acquired based on 200 scans with a time domain of 4 M (mega-points). Before acquisition, the device was externally calibrated with a solution of 0.1 mg/mL arginine (m/z 200–1500) in both ionization modes. The resolution powers were $m/\Delta m_{50\%} = 483,000\text{--}507,000$ for ESI (+) and $m/\Delta m_{50\%} = 382,000\text{--}505,000$ for ESI (–) (where $\Delta m_{50\%}$ is the total width of the peak at the midpoint of its maximum height at m/z 400), and the mass error was < 1 ppm. These settings provided the attributions for the unequivocal molecular formula for individually charged molecular ions. The mass spectra were processed using an algorithm developed specifically for the processing of the signals, the Composer software package (Adermann et al. 2016). The data from the spectra were calibrated, and the elemental composition was determined by measuring the values of m/z . The results were expressed in a graph of class distribution of heteroatomic compounds and a graph of double bond equivalents and rings (DBE) vs the number of carbon atoms to facilitate visualization and interpretation of the MS results. The level of unsaturation of each compound can be deduced from Eq. (2), where the higher the value of DBE, the greater the hydrogen deficiency of the compound:

$$\text{DBE} = \text{C} - (\text{H}/2) + (\text{N}/2) + 1 \quad (2)$$

where C, H, and N are the numbers of carbon, hydrogen, and nitrogen atoms present in the molecule, respectively. The M_w values are provided by the Composer software processing and obey the following formula depicted in Eq. (3):

$$M_w = \frac{\sum_i (N_i M_i^2)}{\sum_i (N_i M_i)} \quad (3)$$

where M_w is the average weight molar mass obtained from the mass spectra, M_i is the m/z value of peak i and N_i is the peak intensity (Santos et al. 2020).

Separation of interfacial material

The IM obtained from oils 1, 2 and 3 were isolated by the method described by Jarvis et al. (2015), which consists of constructing a chromatography column in a 5 mL glass pipette by adding a mixture of 1 g of the sample diluted in heptol (1:1 v/v n-heptane/toluene) and 1 g of silica gel (Fisher Scientific, 70–230 mesh, type 60A) saturated with 66% water (pH ~ 7). The unretained compounds were percolated with an excess of ~ 10 mL of heptol, producing the clean up (CU) fraction (which contains species that are not part of the scope of this work) and, finally, the fraction of interest (IM), which was recovered by elution with ~ 10 mL of toluene/methanol solution (70:30% v/v). Both fractions were dried under N_2 gas until the analytes were solvent-free. No further isolation step was performed.

Results and discussion

Crude oil assay

Table 2 summarizes the crude oil characterization. According to the Brazilian petroleum regulatory agency “Agência Nacional do Petróleo, Gás Natural e Bicomustíveis”, oil 3 with an API gravity 22.0 (see Table 2) is classified as

Table 2 Characteristics of crude oils

Properties	Oil 1	Oil 2	Oil 3
TAN (mg of KOH/g of oil)	1.09	0.40	1.10
Density at 20 $^\circ\text{C}$ ($\text{g}\cdot\text{cm}^{-3}$)	0.8992	0.8830	0.9174
$^\circ\text{API}$ at 15.6 $^\circ\text{C}$	25.1	27.9	22.0
Saturates (wt%)	58.3	59.7	49.8
Aromatics (wt%)	23.4	21.5	29.2
Resins (wt%)	18.0	18.7	19.6
Asphaltenes (wt%)	<0.5 (0.3)	<0.5 (0.1)	1.4
Water (vol%)	0.79	0.20	1.11

heavy and oils 1 and 2 are medium. Oil 3 shows the highest asphaltene content and oils 1 and 3 have higher TAN values.

Dynamic surface tension

The interfacial tension results for oils in the presence of deionized water and saline solutions prepared from each of the three oils are shown in Fig. 2.

Figure 2 shows the results of IFT measured by the pendant drop method as a function of time for oils 1, 2 and 3 in deionized water and different saline solutions. Analyzing the influence of increasing pH on this property, it is apparent that for the less concentrated saline solutions (1 and 2), there was no significant change. On the other hand, for the more concentrated saline solutions (3 and 4), there was a significant change, with a remarkable decrease of IFT for saline solution 4 at pH 8.

Lashkarbolook and Ayatollahi (2018a, b) reported that the IFT is maximum when the pH is close to neutral, i.e., the IFT is reduced when the pH is either decreased or increased. It can be seen in Fig. 2a that the oil phase in contact with

deionized water (DI), which has a pH close to neutral, showed a higher IFT compared to the other experimental conditions (brines 1, 2, 3 and 4). Looking at the behavior of IFT vs. time for brine 1 (lower pH, 6), one initially notices the highest IFT in the first 5000 s, eventually reaching an IFT close to 22 mN m^{-1} , similar to brine 2 (upper pH, 8). However, the difference in IFT became more pronounced between brines 3 and 4, which are more concentrated; brine 3 (lower pH, i.e. pH 6) initially obtained a higher IFT in the first 500 s and thereafter remained practically constant with an IFT around 19 mN m^{-1} , in contrast to brine 4 (pH 8), which reached lower IFT values, ranging between 15 and 13 mN m^{-1} and remained constant in the first 500 s. This demonstrates that the influence of the concentration of salts in the system is crucial to reduce interfacial tension, which is further aided for oil 1 by increasing the pH.

Figure 2b, c show the IFT per drop plots versus time for oil 2 and oil 3, respectively, submitted to DI and different saline solutions. The oil phase in contact with deionized water presented higher IFT values in relation to the other experimental conditions (brines 1, 2, 3 and 4), as expected. However, when comparing the oil/DI behavior of the three oils, it was observed that the IFT values are higher for oil 3 (Fig. 2c), which has a greater concentration of resins and asphaltenes because it is more active at the oil/DI interface due to its hydrophilic behavior.

In general, by looking at each brine individually, it is possible to note that the variation of the IFT in relation to each oil was small. Only for brine 3 (which has a higher salt

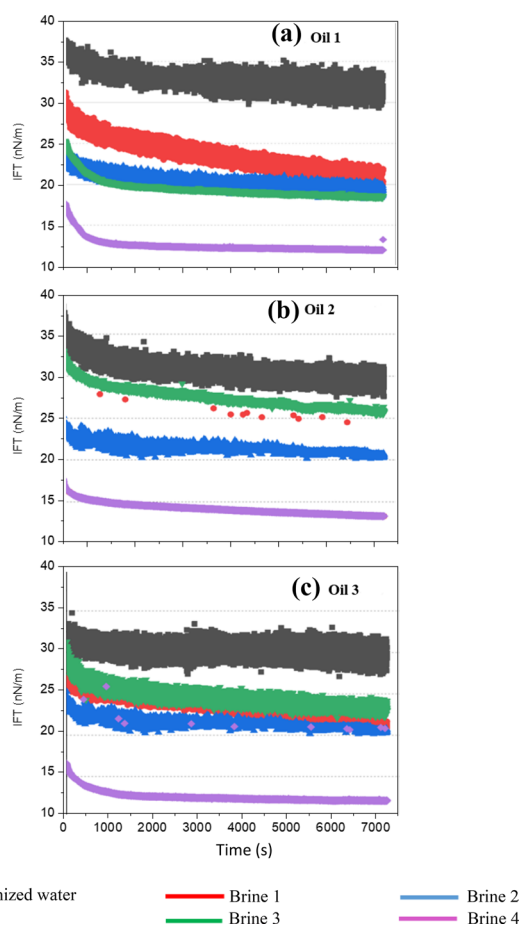


Fig. 2 Interfacial tension evolution with time for the different oils in the presence of deionized water and saline solutions (see Table 1)

Table 3 ^1H and ^{13}C NMR assignments (molar %)

*Symbol	Oil 1	Oil 2	Oil 3
Hdar	2.3	2.0	2.9
Hmar	2.3	1.7	2.6
Har	4.6	3.8	5.5
Holf	<0.1	<0.1	<0.1
Halfa	8.6	7.5	10.6
H β -1	14.1	12.8	14.8
H β -2	43.3	48.0	40.8
H γ	29.2	27.8	28.1
Hsat	95.3	96.1	94.4
Car-alk	6.2	4.8	7.4
Car-H	8.3	6.9	9.7
Car-b (Car-ar + Car-ar- ar + Car-Me)	4.1	3.7	5.1
Car tot	19.6	16.7	23.4
Csat	80.4	83.3	76.6
Cmet-term	4.1	4.8	3.7
Cmet-bran	8.4	7.0	8.5
Average linear chain length (in carbon atoms)	12	14	11

*Symbols according to reference (Chinelatto Jr et al. 2018)

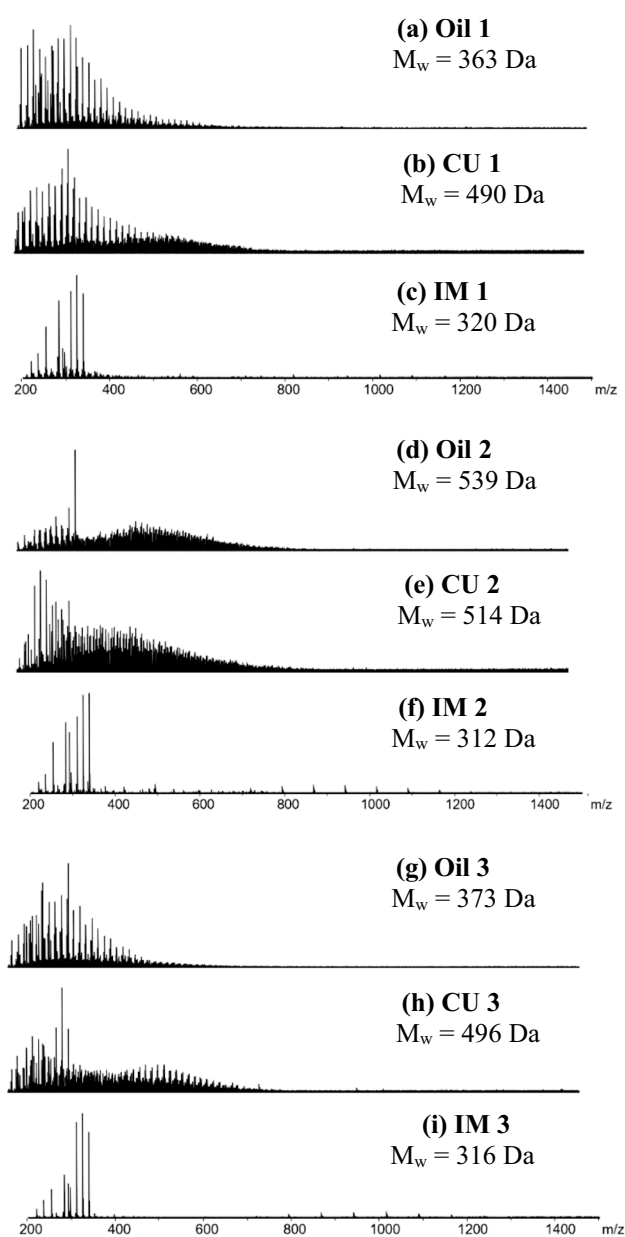


Fig. 3 ESI(-)FT-ICR MS spectra of crude oils 1–3 and their CUs and IMs

concentration and a pH of 6) subjected to oil 2 and oil 3, was there an increase in the IFT. The literature reports that IFT values decrease with increasing TAN (Lashkarbolook and Ayatollahi 2018a, Lashkarbolook and Ayatollahi 2018b), which may explain the significant increase in IFT for oil 2, which has a higher content of saturates (59.7%), lower resin and asphaltene content (18.7 and <0.5% m/m respectively) and lower acidity (~ 0.4 mg KOH g^{-1}). Lashkarbolook and Ayatollahi (2018a and 2018b) explain that the presence of amphoteric materials (resins and asphaltenes) can cause a reduction in IFT values and that this reduction may be accentuated with increasing pH, as it favors the dissociation of

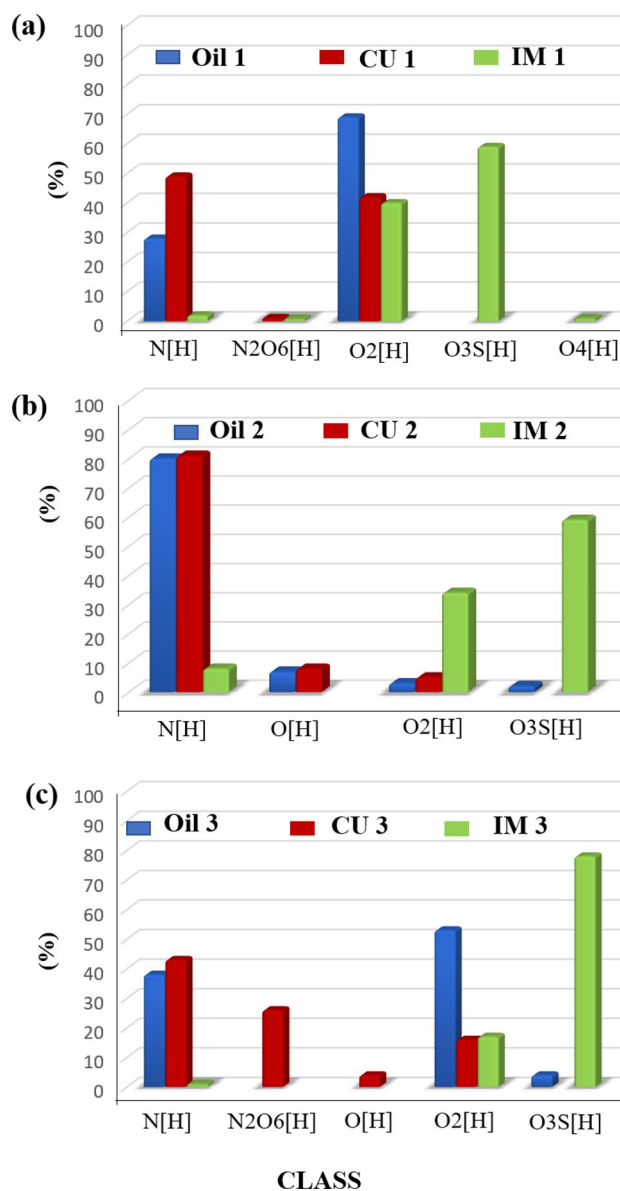


Fig. 4 Class distribution obtained from ESI(-)FT-ICR MS data for crude oils 1–3 and their CUs and IMs

asphaltenes. Thus, brine 3 subjected to oil 1 (TAN ~ 1.1 mg KOH g^{-1}) had an increase in IFT in relation to oil 3, with the same acidity, but with a higher content of resins and asphaltenes.

Another important observation was that the systems with smaller amounts of salt needed less time for interfacial film formation relative to a system containing higher saline concentrations (Verruto et al. 2009). This was seen by comparing the behavior of the curves of oil 1 for brines at the same pH and different salt concentrations (Fig. 2); comparing brine 1 with brine 3 (both at pH 6 and with lower and higher salt concentrations, respectively). It is noted that brine 1 (lower salinity) shows higher IFT values. The

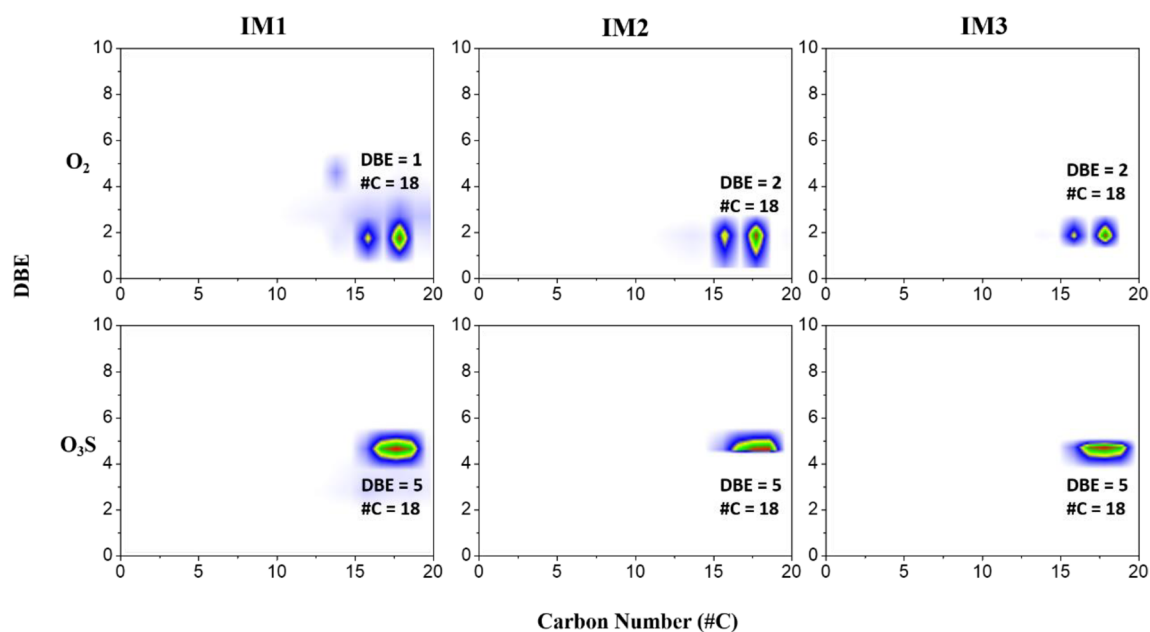


Fig. 5 DBE versus carbon number (#C) of the O₂ and O₃ classes present in the IM

same phenomenon was observed between brines 2 and 4 (both at pH 8 and with lower and higher salt concentrations, respectively). For oil 2 and oil 3, this behavior was repeated only between brines 2 and 4. In this context, the literature reports that the presence of electrolytes causes significant changes in the dynamics of interfacial film formation (Verruto et al. 2009). However, the reduction in the kinetics of interfacial film formation in salt-containing systems is the result of three interconnected mechanisms that depend on the chemical nature of asphaltenes: (1) attraction between the electrolytes present in the aqueous phase and the asphaltenes; (2) increased concentration of asphaltenes in the interfacial film, resulting from the electrostatic interactions between these and the electrolytes and (3) the formation of a film with low consolidation capacity composed of continuously adsorbed asphaltenes (Verruto et al. 2009). In this way, the chemical nature of the asphaltenes present in oil 2 and oil 3 may account for the non-repetition of this behavior between brines 1 and 3.

NMR characterization

The molar percentage of H and C species obtained by ¹H and ¹³C NMR spectra for the oils are shown in Table 3. The NMR spectra can be analyzed by carefully observing the aliphatic and aromatic regions according to the literature (Hasan et al. 1983; Jennings et al. 1993). Oil 3, with the highest asphaltene, resin and aromatic content, shows the highest number of aromatic hydrogens linked to carbons in

monoaromatic rings (H_{mar}) and polyaromatic rings (H_{dar}), in agreement with its lower API gravity.

Oil 3 has the highest degree of bridgehead carbons (Car-b), as expected by its higher degree of aromatics and asphaltenes (see Table 2). In the aliphatic region of the ¹H NMR spectra, H_β-2 is higher than H_β-1 for all samples. This is an indication that paraffinic hydrogens in long alkyl chains attached to aromatic rings are higher than naphthenic hydrogens and paraffinic hydrogens in short alkyl chains attached to aromatic rings. The average linear chain length (in carbon atoms) in Table 3 indicates that oil 2 is more paraffinic.

ESI(±)FT-ICR MS characterization

Figure 3 shows the ESI(-)FT-ICR mass spectra for oils 1 to 3, and their CUs and IMs. It is apparent that the species found in the MI samples showed lower M_w values than their respective CU. All FT-ICR mass spectra—referring to samples of interfacial materials (Fig. 3c, f, i)—present an important reduction in the *m/z* range (from 200–350 for IM 1, IM 2 and IM 3) and M_w, (IM 1 [320 Da], IM 2 [312 Da] and IM 3 [316 Da]), in relation to their respective oils of origin: Oil 1 (Fig. 3a, *m/z* 200–700 and 363 Da), Oil 2 (Fig. 3d, *m/z* 200–900 and 539 Da) and Oil 3 (Fig. 3g, *m/z* 200–600 and 373 Da).

On other hand, there was an increase in *m/z* intervals in the FT-ICR mass spectra of samples from the clean up steps; CU 1 (Fig. 3b) and CU 3 (Fig. 3h), both had *m/z* values between 200 and 800, and the *m/z* of CU 2 was between 200

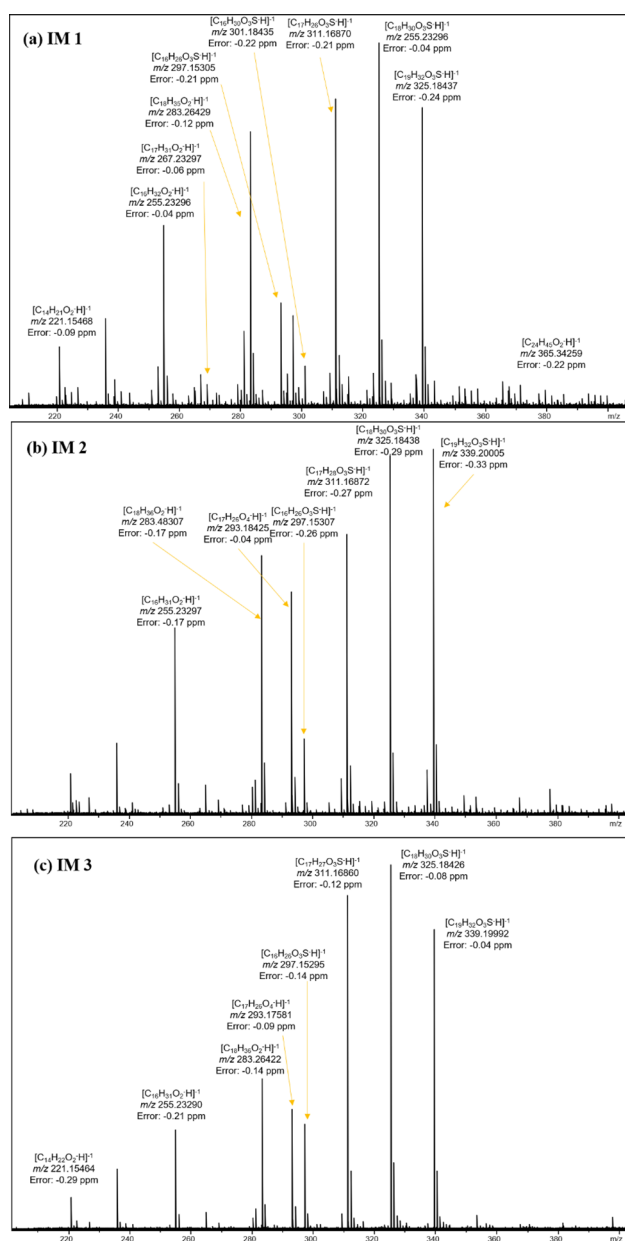


Fig. 6 Magnification of ESI(-)FT-ICR mass spectra of IMs 1–3 in the m/z 200–400 region highlighting the detection of $O_3S[H]$, $O_2[H]$, and $O_4[H]$ classes

and 900 (Fig. 3e), in relation to the mass spectra of their respective oils of origin. This outcome occurred because ESI preferentially ionizes polar species with higher pK_b and lower M_w values (Barros et al. 2017).

To aid interpretation of the results, histograms of the relative percentages of the classes of compounds present in oils 1, 2 and 3, and their respective CUs and IMs identified by ESI(-)FT-ICR MS were produced (Fig. 4). The neutral N class found in ESI(-)FT-ICR mass spectra, are abundant in the three oil samples and their respective CU fractions,

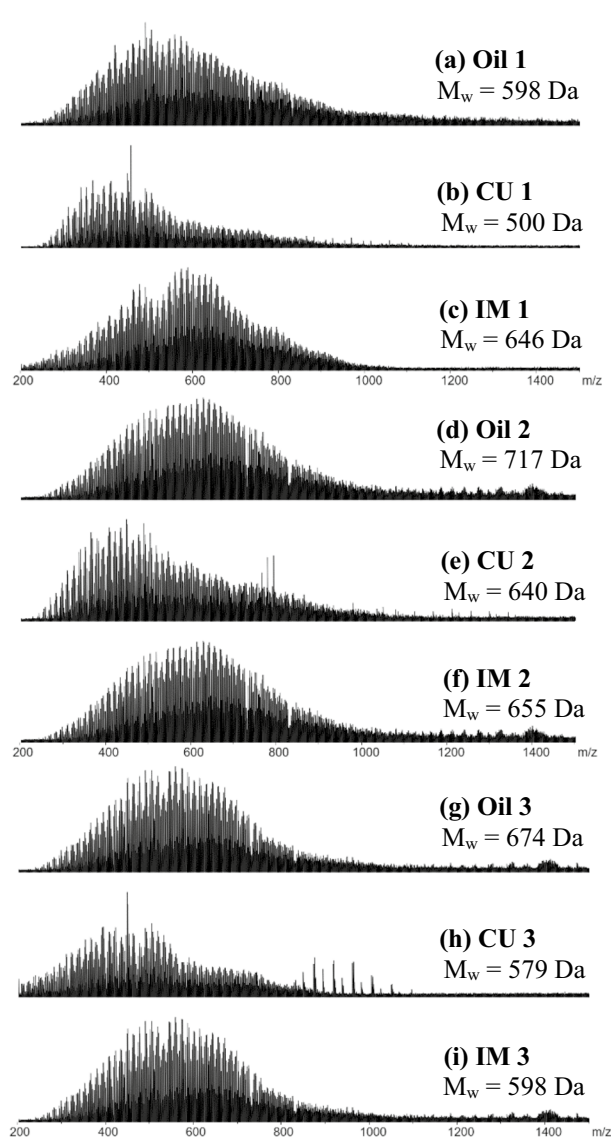


Fig. 7 ESI(+)-FT-ICR MS spectra of crude oils 1–3 and their CUs and IMs

while acidic $O_2[H]$ and mixed $O_3S[H]$ are the more abundant classes in the IMs (Fig. 4).

Unsurprisingly, the $O_2[H]$ class, presumably due to the presence of carboxylic acids, was the most abundant class in oils 1 and 3, with higher TAN values (see Fig. 4 and Table 2). However, some non-interfacially active class $O_2[H]$ remained in the CUs. Although oil 2 had the lowest TAN value, its IM had a more abundant class $O_2[H]$ than in the parent oil. The most abundant $O_3S[H]$ species in IMs have a continuum distribution from C_{14} to C_{24} with DBE ranging from 1 to 5. The most abundant structures are $[C_{17}H_{28}O_3S-H]^{-1}$, $[C_{18}H_{30}O_3S-H]^{-1}$ and $[C_{19}H_{32}O_3S-H]^{-1}$ (DBE = 4 in all cases), suggestive of surfactants naturally

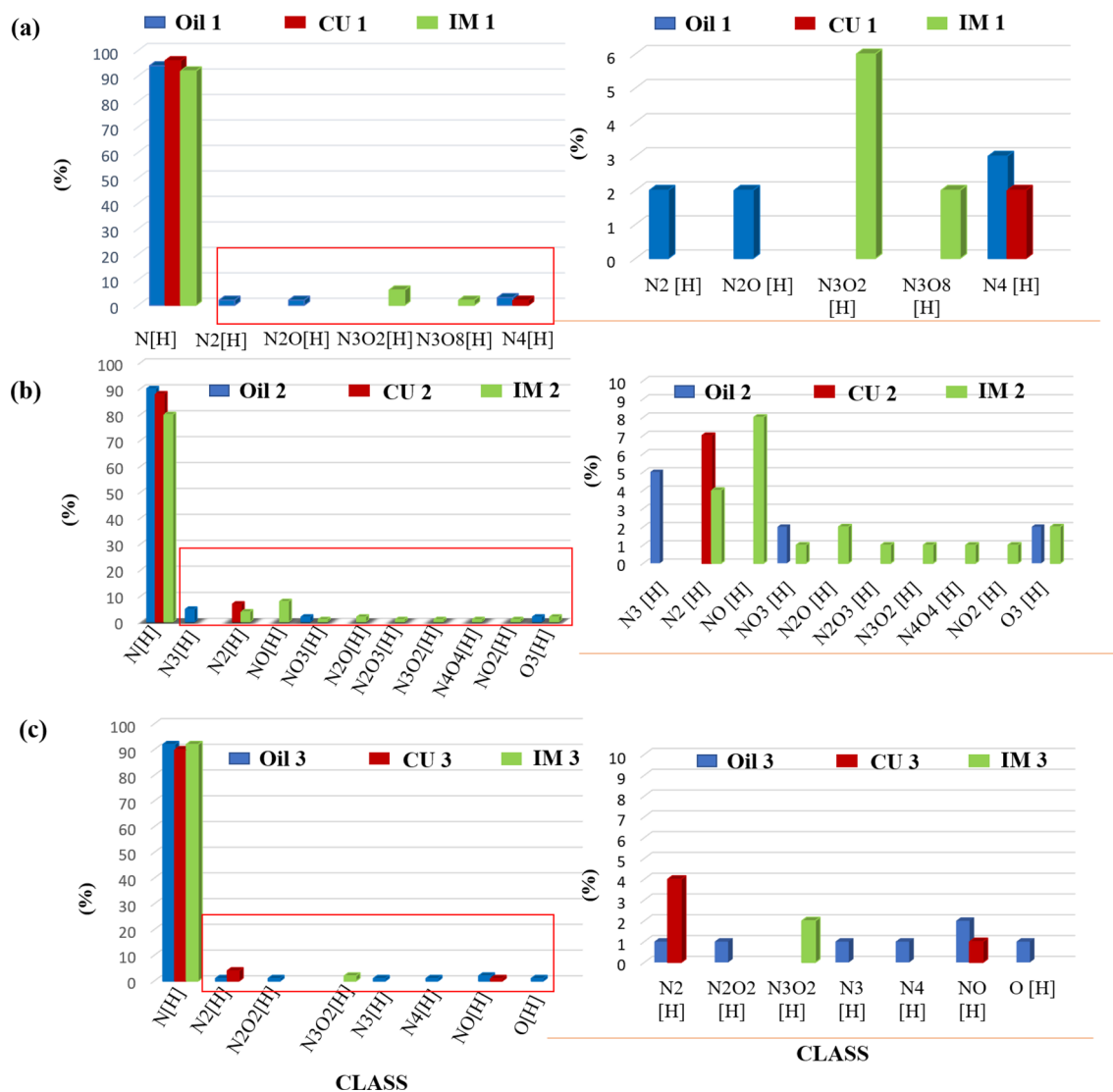


Fig. 8 Class distribution obtained from ESI(+)-FT-ICR MS data for crude oils 1–3, their CUs and IMs (left panels) and their respective expansions (right panels)

present in petroleum, likely thiophenic carboxylic acids (see Fig. 5). Anthropogenic chemical products such as surfactants artificially added to crude oils to alter wetting characteristics do not span such a wide range of carbon-number and DBE at the same time (Chegenizadeh et al. 2017). For instance, linear alkylbenzene sulfonates are the most common surfactants used commercially and domestically in the detergent industry and have a discrete DBE of 4 (Stanford et al. 2007). Due to $O_3S[H]$ class amphiphilic behavior, these species can be adsorbed and orient themselves spontaneously and interfere with the behavior of the W/O interface (Lalli et al. 2017). Nonetheless, Wu et al. (2022), in their analysis of MS/MS spectra from ESI(-) Orbitrap MS data of $[C_{18}H_{30}O_3S-H]^{-1}$ detected in the IM from Daqing oil, observed no obvious fragment losses of H_2O and CO_2 , or

$O_3S[H]^{-1}$ in the MS spectrum. The authors suggested that the $O_3S[H]$ class in the IM from the Daqing crude oil was predominantly alkylbenzene sulfonates, which are artificially synthesized chemicals added during the large-scale enhanced oil recovery process implemented in this oilfield.

Figure 7 displays the ESI(+)-FT-ICR MS spectra of three crude oils. The profiles for crude oils 2 and 3 were quite similar, with maxima at m/z 717 and 674 Da, respectively. Crude oil 1 showed a maximum at 598 Da. The CU extracted compounds had lower molecular weight values.

The presence of the $O_2[H]$ class in the composition of these IMs confirms the participation of carboxylic acids in the stabilization of W/O for the studied oils. The class distribution obtained by ESI(+)-FT-ICR MS (Fig. 8) reveals that the N[H] class was the most abundant in all the oils and

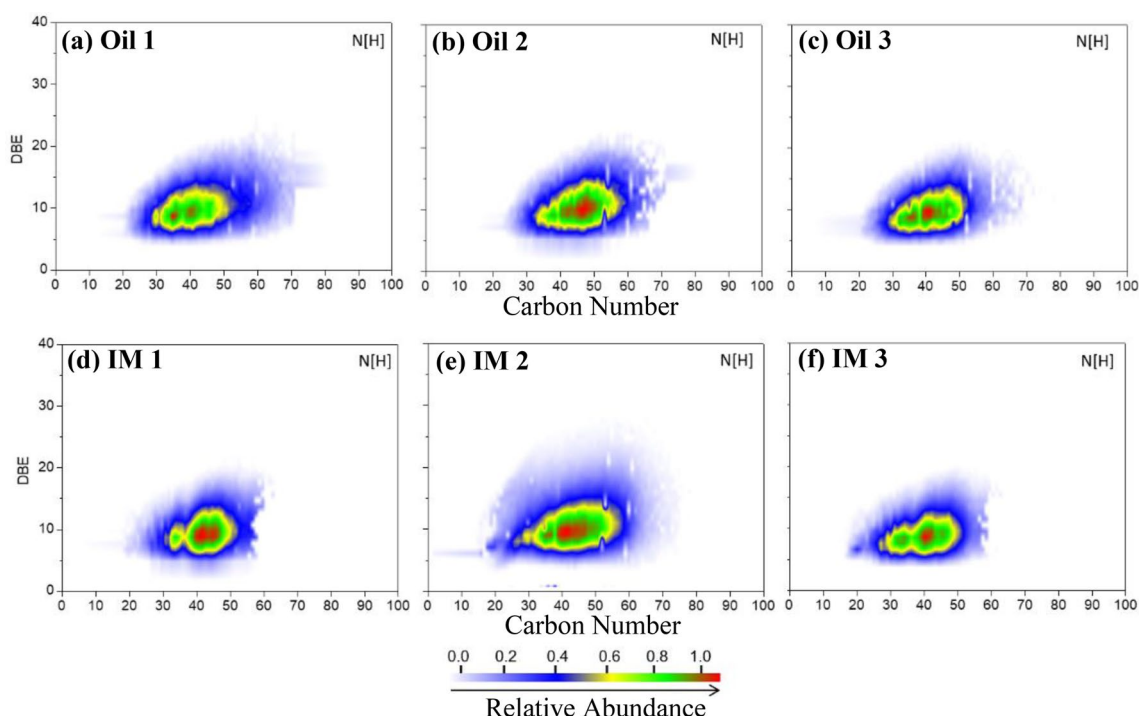


Fig. 9 Graphs of DBE vs carbon number for class N[H] plotted with data from ESI(+)-FT-ICR MS for crude oils 1–3 and their IMs

its fractions, having pyridine as the basic structure forming its components. This profile of N[H] class predominance when applying ESI(+)-FT-ICR MS is commonly observed in studies of crude oil due to the more efficient ionization of the pyridine compounds versus the other classes, resulting from the greater basicity of these compounds in solution. Only subtle differences were observed in the compositions of the crude oils and their fractions (Pereira et al. 2014).

To facilitate the interpretation of the compositional trends, three-dimensional plots of DBE (y-axis) versus carbon number (x-axis), with the relative abundance represented by a color scale for the N[H] class are presented in Fig. 9. Therefore, in the DBE versus CN plot for a particular heteroatom class, compounds that belong to the same homologous series have equal DBE (rings and double-bonds), but different CN (CH_2 units). Data from ESI(+)-FT-ICR MS (see Fig. 9) demonstrates a continuum distribution from C_{15} to C_{70} carbon atoms (maximum around C_{40}) with DBE from 7 to 15 (maximum around 9) for the three IMs, which suggests the presence of aromatic rings.

Collectively, the results highlight the existence of poly-functional, interfacially active molecules capable of interacting in the W/O interface through several intermolecular forces, including hydrogen bonding between nitrogen and oxygen-containing functionalities, π -stacking of aromatic cores, acid/base interactions between carboxylic acids and pyridine rings, and London dispersion forces between aliphatic moieties. This demonstrates that the ESI(\pm)-FT-ICR

MS (Figs. 3, 4, 5, 6, 7, 8, 9) provided additional and detailed information that was not observed in the SARA analysis of crude oils (Table 2) or the NMR data for the oils (Table 3).

Conclusions

The chemical characterization of IMs isolated from three different crude oils by the wet silica method revealed their polar, aromatic and higher molecular weight hydrocarbon compositions. These molecules are adsorbed onto the hydrophilic surface of the silica particles. The CU fractions, containing the particles that were not adsorbed on the silica particles, had a predominantly lower molecular weight hydrocarbon composition. Based on the wet silica method, the sulfonate $\text{O}_3\text{S}[\text{H}]$ classes, presumably of endogenous origin, and $\text{O}_2[\text{H}]$ have a surface-active character because they are retained over aqueous media. The N[H] class is abundant in the three crude oils and their CUs and IMs, probably due to the more efficient ionization of the pyridine compounds versus the other chemical species. The IMs contain an abundance of molecules crowded with heteroatoms showing at least one pair of non-bonding valence shell electrons (i.e., N, O and S) suggesting that hydrogen bonding is pivotal in stabilizing the W/O emulsions, as previously reported in the literature (Ma et al. 2021). Other intermolecular forces, such as acid/base interactions between carboxylic

acids and nitrogen bases, may play an important role in emulsion stabilization as these two classes were detected in the isolated IMs.

The characterization described in the present work may provide key information for developing new methods for the treatment of W/O emulsions, reducing or mitigating flow assurance issues.

We intend to carry out further studies under different conditions to evaluate the IFT of the IM and CU fractions isolated and characterized in the present work to better understand the multi-factor synergistic emulsification stabilization mechanism.

Acknowledgements The authors would like to thank CENPES/PETROBRAS (process No. 2018/00110-4) for funding the research. The authors thank Professor Zhenghe Xu from the Department of Chemical and Materials Engineering (University of Alberta, Canada) and Dr. Heloisa Pinto Dias for dynamic surface tension analyses. The authors thank the Federal Institute of Espírito Santo (IFES, ES, Brazil) for the financial support. The authors also thank the Labpetro (UFES, ES, Brazil), the Characterization Laboratory and Petroleomic and Forensics Laboratory.

Data availability Data supporting the findings of this study are available within the article. Additionally, raw data are available on request from the corresponding author.

Declarations

Conflict of interest The authors declare no competing financial interest.

References

- ASTM D6560–17 – Standard Test Method for Determination of Asphaltenes (Heptane Insolubles) In Crude Oil Petroleum and Petroleum Products.
- ASTM D664–18 - Standard Test Method for Acid Number of Petroleum Products by Potentiometric Titration.
- ASTM D4377–20 - Standard Test Method for Water in Crude Oils by Potentiometric Karl Fischer Titration.
- Adermann N, Boggiano J, Composer, version 1.5.3; Sierra Analytics, Pasadena, CA, USA, 2016.
- Barros EV, Dias HP, Pinto FE, Gomes AO, Moura RR, Sad CMS, Freitas JCC, Neto Cunha A, AQUIJE GMFV, Romão W (2017) Study of degradation of acid crude oil by high resolution analytical techniques. *J Petrol Sci Eng* 154:194–203. <https://doi.org/10.1016/j.petrol.2017.04.032>
- Berry JD, Neeson MJ, Dagastine RR, Chan DYC, Tabor RF (2015) Measurement of surface and interfacial tension using pendant drop tensiometry. *J Colloid Interface Sci* 454:226–237. <https://doi.org/10.1016/j.jcis.2015.05.012>
- Bertheussen A, Simon S, Sjöblom J (2018) Equilibrium partitioning of naphthenic acid mixture part 2: Crude oil extracted naphthenic acids. *Energy Fuels* 32(9):9142–9158. <https://doi.org/10.1021/acs.energyfuels.8b01870>
- Chegenizadeh N, Saeedi A, Quan X (2017) Most common surfactants employed in chemical enhanced oil recovery. *Petroleum* 3:197–211. <https://doi.org/10.1016/j.petlm.2016.11.007>
- Czarnecki J, Tchoukov P, Dabros T (2012) Possible role of asphaltenes in the stabilization of water-in-crude oil emulsions. *Energy Fuel* 26:5782–5786. <https://doi.org/10.1021/ef300904a>
- Ese MH, Kilpatrick PK (2004) Stabilization of water-in-oil emulsions by naphthenic acids and their salts: model compounds, role of pH, and soap: acid ratio. *J Dispersion Sci Technol* 25:253–261. <https://doi.org/10.1081/DIS-120038634>
- Facanali R, NdeA P, Crucello J, Carvalho RM, Vaz BG, Hantao, (2021) Naphthenic acids: formation, role in emulsion stability, and recent advances in mass spectrometry-based analytical methods. *J Anal Methods Chem* 2021:1–9. <https://doi.org/10.1155/2021/6078084>
- Hasan MU, Ali MF, Bukhari A (1983) Structural characterization of Saudi Arabian heavy crude oil by n.m.r. spectroscopy. *Fuel* 62:518–523. [https://doi.org/10.1016/0016-2361\(83\)90219-3](https://doi.org/10.1016/0016-2361(83)90219-3)
- He L, Lin F, Li X, Sui H, Xu Z (2015) Interfacial sciences in unconventional petroleum production: From fundamentals to applications. *Chem Soc Rev* 44:5446–5494. <https://doi.org/10.1039/C5CS00102A>
- ISO 12185–96 – Crude petroleum and petroleum products – Determination of density – Oscillation U-tube method.
- Jarvis JM, Robbins WK, Corilo YE, Rodgers RP (2015) Novel method to isolate interfacial material. *Energy Fuels* 29:7058–7064. <https://doi.org/10.1021/acs.energyfuels.5b01787>
- Jennings PW, Pribanic JA (1993) Binder Characterization and Evaluation by Nuclear Magnetic Resonance Spectroscopy; Strategic Highway Research Program, National Research Council: Washington, D.C., SHRP-A-335. <http://onlinepubs.trb.org/onlinepubs/shrp/SHRP-A-335.pdf>
- JrLS C, Menezes SMC, HdeA H, de Oliveira MCK, Marques LCC (2018) Diffusion-ordered spectroscopy nuclear magnetic resonance as an alternative technique to improve asphaltene characterization. *Energy Fuels* 32(3):2793–2800. <https://doi.org/10.1021/acs.energyfuels.7b02973>
- Lalli PM, Jarvis JM, Marshall AG, Rodgers RP (2017) Functional Isomers in Petroleum Emulsion Interfacial Material Revealed by Ion Mobility Mass Spectrometry and Collision-Induced Dissociation. *Energy Fuels* 31:311–318. <https://doi.org/10.1021/acs.energyfuels.6b02411>
- Lashkarbolooki M, Ayatollahi S (2018a) Effects of asphaltene, resin and crude oil type on the interfacial tension of crude oil/brine solution. *Fuel* 223:261. <https://doi.org/10.1016/j.fuel.2018.03.029>
- Lashkarbolooki M, Ayatollahi S (2018b) The effects of pH, acidity, asphaltene and resin fraction on crude oil/water interfacial tension. *J Petrol Sci Eng* 162:341–267. <https://doi.org/10.1016/j.petrol.2017.12.061>
- Li D, Gao B, Cui X (2022) Emulsifying behavior between oil and water of flowback fluids from acidizing oil wells based on high-voltage electric field oil–water separation technology. *New J Chem* 46:16858. <https://doi.org/10.1039/D2NJ02306G>
- Li Z, Fuentes J, Chakraborty A, Zamora E, Prasad V, Vázquez F, Xu Z, Liu Q, Flores C, McCaffrey WC (2023) Dehydration of water-in-crude oil emulsions using polymeric demulsifiers: a model for water removal based on the viscoelastic properties of the oil–water interfacial film. *Fuel* 332:126185. <https://doi.org/10.1016/j.fuel.2022.126185>
- Ma J, Yang Y, Li X, Sui H, He L (2021) Mechanisms on the stability and instability of water-in-oil emulsion stabilized by interfacially active asphaltenes: Role of hydrogen bonding reconstructing. *Fuel* 297:120763. <https://doi.org/10.1016/j.fuel.2021.120763>
- Mahavadi SC, Al Hamad M, Ma SM, Abdallah W (2022) Role of polar species in determining the interfacial tension of a crude oil/water system. *Energy Fuels* 36(16):8769–8777. <https://doi.org/10.1021/acs.energyfuels.2c00557>
- Pereira RCL, Carvalho RM, Couto BC, de Oliveira MCK, Eberlin M, Vaz BG (2014) Wax crude oil emulsion gel: chemical

- characterization of emulsified phase extract components. *Energy Fuels* 28(12):7352–7358. <https://doi.org/10.1021/ef500962e>
- Santos JM, Vetere A, Wisniewski A, Eberlin MN, Schrader W (2020) Modified SARA method to unravel the complexity of resin fraction(s) in crude oil. *Energy Fuels* 34(12):16006. <https://doi.org/10.1021/acs.energyfuels.0c02833>
- Schabron JF, Jr JF R, Sanderson MM (2010) Asphaltene determinant method for automated on-column precipitation and redissolution of pericondensed aromatic asphaltene components. *Energy Fuels* 24(11):5984–5996. <https://doi.org/10.1021/ef100822f>
- Soares IF, de Oliveira MCK, Naccache MF, Nele M (2021) Effects of monovalent and divalent cations on the rheology of organic acid laden interfaces. *J Dispersion Sci Technol* 18:1–13. <https://doi.org/10.1080/01932691.2021.2017296>
- Spiecker PM, Gawrys KL, Trail CB, Kilpatrick PK (2003) Effects of petroleum resins on asphaltene aggregation and water-in-oil emulsion formation. *Colloids Surf A* 220(1–3):9–27. [https://doi.org/10.1016/S0927-7757\(03\)00079-7](https://doi.org/10.1016/S0927-7757(03)00079-7)
- Stanford LA, Kim S, Lein GC, Smith D, Rodgers RP, Marshall AG (2007) Identification of water-soluble heavy crude oil organic-acids, bases, and neutrals by electrospray ionization and field desorption ionization fourier transform ion cyclotron resonance mass spectrometry. *Environ Sci Technol* 41:2696–2702. <https://doi.org/10.1021/es0624063>
- Tchoukov P, Yang F, Xu Z, Dabros T, Czarnecki J, Sjöblom J (2014) Role of asphaltenes in stabilizing thin liquid emulsion films. *Langmuir* 30(11):3024–3033. <https://doi.org/10.1021/la404825g>
- Verruto VJ, Le KR, Kilpatrick PK (2009) Adsorption and molecular rearrangement of amphoteric species at oil-water interfaces. *J Phys Chem B* 113:13788. <https://doi.org/10.1021/jp902923j>
- Wong SF, Lim JS, Doi SS (2015) Crude oil emulsion: a review on formation, classification and stability of water-in-oil emulsions. *J Petrol Sci Eng* 135:498–504. <https://doi.org/10.1016/j.petrol.2015.10.006>
- Wu X (2003) Investigating the stability mechanism of water-in-diluted bitumen emulsions through isolation and characterization of the stabilizing materials at the interface. *Energy Fuels* 17(1):179–190. <https://doi.org/10.1021/ef020098y>
- Wu J, Li H, Zhao Q, Zhou B, Lun Z, Zhang Y, Chung KH, Shi Q (2022) Characterization of crude oil interfacial material by high-resolution mass spectrometry. *J Petrol Sci Eng* 214: 110509. <https://doi.org/10.1016/j.petrol.2022.110509>

Publisher's Note Springer Nature remains neutral with regard to jurisdictional claims in published maps and institutional affiliations.

Springer Nature or its licensor (e.g. a society or other partner) holds exclusive rights to this article under a publishing agreement with the author(s) or other rightsholder(s); author self-archiving of the accepted manuscript version of this article is solely governed by the terms of such publishing agreement and applicable law.